2011 American Control Conference
on O'Farrell Street, San Francisco, CA, USA
June 29 - July 01, 2011

Macroscopic Mechanistic Modeling and Optimization of a Self-Initiated High-Temperature Polymerization Reactor

Thomas Rier, Sriraj Srinivasan, Masoud Soroush, George A. Kalfas, Michael C. Grady, and Andrew M. Rappe

Abstract— **This paper presents a macroscopic mechanistic mathematical modeling and optimization study of a batch polymerization reactor in which self-initiated free-radical polymerization of n-butyl acrylate at 140 and 160°C takes place. The model is obtained using a comprehensive free-radical polymerization reaction mechanism. The rate constant of the monomer self-initiation is estimated from monomer conversion measurements. The model is validated using a different set of conversion measurements. The validation results show that the macroscopic mechanistic model is accurate enough for optimization of the self-initiated polymerization reactor to produce high quality acrylic resins. The model is then used to calculate an optimal batch-reactor temperature profile that yields an end-batch polymer product with desired properties (conversion and number-average molecular weight).**

I. Introduction

Acrylic resins are widely used in automobile paint and coating formulations as weather-proofing agents and constitute a multi-billion dollar global market that is continuously growing [1], [2]. In the last several decades, because of stringent environmental regulations in North America, the volatile organic content in paints and coatings has been reduced to less than 300 g/l [3]. Acrylic resins with high molecular weight and high solvent content were replaced with low molecular weight, low solvent content resins. High-temperature (greater than $100°C$) free-radical polymerization processes were developed to produce these resins in place of conventional low-temperature polymerization processes.

Initiators such as organic peroxides and azonitriles have been commonly used to initiate high-temperature polymerization of alkyl acrylates, but their high costs and tendency to produce coloration when they are left unreacted in the end-product have made them less attractive to use [4], [5]. Spontaneous thermal polymerization of alkyl acrylates was found to take place in the absence of any known added external initiators [6]. Such a process could provide an attractive alternative for the production of low molecular weight polymers of alkyl acrylates. Initial studies [7], [8] using electronspray ionization-Fourier transform mass spectrometry (ESI-FTMS), nuclear magnetic resonance (NMR) spectroscopy and detailed analytic macroscopic modeling were unable to reveal the true nature of the initiating species and the mechanism of initiation. More recently, using quantum chemical calculations [9], [10], it has been shown that monomer self-initiation in alkyl acrylate polymerization is the dominant initiating mechanism. Further evidence to the occurrence of the self-initiation mechanism was shown by accurately fitting the computed structures to matrix-assisted laser desorption ionization-time of flight mass spectrometry [11] and ESI-FTMS spectrum [12] of poly-alkyl acrylate samples that were generated using the spontaneous thermal polymerization process.

Macroscopic kinetic models are important tools to understand complex polymerization processes [12], [13]. The influence of various parameters on the overall kinetics and thermodynamics of the process can be identified with the development of reasonably accurate mechanistic models. The advantage of mechanistic over semi-empirical models is in their ability to account for the rate constants of individual reactions and provide information about the impact of each of these reactions on the overall polymerization kinetics [14]. Also, the kinetics computed using quantum chemical calculations can be used in the mechanistic models to improve the prediction of variables such as monomer conversion, average molecular weights and chain branches per 100 monomer units [15]. A macroscopic model can be used to calculate optimal reactor operating conditions, design model-based controllers, conduct experimental design, and design products with improved quality [16]. A macroscopic mechanistic model can be developed using several approaches. The black box approach is based upon empirical correlations that are obtained via well-designed experiments, but have limited predictive power. On the other hand, the detailed analytic approach is capable of describing the composition of polymer mass at any time instant by using the information about elementary kinetic mechanisms. However, the lack of adequate quantitative knowledge on many individual reactions in a polymerization process has limited the prediction capabilities of the detailed analytical models. A third modeling method is that of tendency modeling, in which number of monomer units in polymer chains is not accounted for, and the Schulz-Flory distribution is used to obtain the moments of live and dead polymer chains. While this simplification reduces the complexity involved in solving the model equations,

T. Rier, S. Srinivasan and M. Soroush are with the Department of Chemical and Biological Engineering, Drexel University, Philadelphia, PA 19104, U.S.A.

G.A. Kalfas and M.C. Grady are with DuPont Experimental Station, Wilmington, DE 19880, USA

A.M. Rappe is with Makineni Theoretical Laboratories, Department of Chemistry, University of Pennsylvania, Philadelphia, PA, USA

Corresponding author: M. Soroush; 215-895-1710 (phone); 215-895-2227 (fax); ms1@drexel.edu

This work was supported by the National Science Foundation Grant CBET–0932882.

the tendency modeling approach provides little information on the individual radicals and their chain length during polymerization [17].

Propagation rate constants in free-radical polymerization of styrene, methyl methacrylate and alkyl acrylates have been measured through pulsed laser polymerization-size exclusion chromatography (PLP-SEC) technique [18], [19], [20]. Because this technique is unable to accurately determine rate constants at high temperatures, alternative methods should be used for the estimation of the rate constants in high-temperature polymerization. One of these alternative methods is macroscopic kinetic modeling combined with estimation of the reaction rate constants from measurements obtained from polymer sample analyses [8]. Previous macroscopic mechanistic modeling studies of spontaneous thermal polymerization of styrene and methyl methacrylate have provided qualitative evidence to the occurrence of self-initiation [21], [22]. Styrene and methyl methacrylate self-initiation rate constants have been reported [22], [8] to have an order greater than two. Extensive studies of macroscopic kinetic modeling of high-temperature polymerization of alkyl acrylates, initiated by added thermal initiators, have reported rate constants of various reactions [8], [23]. Rantow et al. [8] explored spontaneous polymerization of n-butyl acrylate using a detailed analytic modeling approach and were able to predict the activation energy and rate constants of spontaneous initiation, backbiting and β-scission reactions. However, no fundamental understanding of the initiation mechanism was obtained from this study.

In this paper, a macroscopic mechanistic kinetic model is developed for self-initiated polymerization of n-butyl acrylate (nBA) in a batch reactor. The rate constant of the self-initiation reaction is estimated from monomer conversion measurements, and the model is validated using a different set of measurements. The model is then used to calculate an optimal temperature profile for a batch polymerization reactor.

The organization of the rest of this paper is as follows. Section II describes the development of the mathematical model. Section III discusses the parameter estimation. Section IV presents the optimization study. Finally, concluding remarks are given in Section V.

II. Mathematical Modeling

A. Reaction Mechanisms

The reaction scheme considered here for thermally self-initiated free-radical polymerization of nBA involves the following reactions (Table 1): thermal self-initiation, chain propagation, intra-molecular chain transfer to polymer (backbiting), inter-molecular chain transfer to polymer, chain transfer to solvent, and chain transfer to monomer, β-scission, termination by disproportionation and termination by combination.

Here, M and S represent the monomer and solvent, respectively. D_n denotes a dead polymer chain with n monomer units but without a terminal double bond. U_n is a dead polymer chain with n monomer units and a terminal

TABLE I
Reaction Mechanisms

a. Monomer self-initiation reactions

$$3M \xrightarrow{k_i} R_1^* + R_2^*$$

b. Propagation reactions

$$R_n^* + M \xrightarrow{k_p} R_{n+1}^*$$
$$R_n^{**} + M \xrightarrow{k_p^t} R_{n+1}^* \quad \text{(+LCB)}$$
$$R_n^{***} + M \xrightarrow{k_p^t} R_{n+1}^* \quad \text{(+SCB)}$$
$$R_n^* + U_m \xrightarrow{k_{mac}} R_{n+m}^{**}$$

c. Backbiting reactions ($n > 2$)

$$R_n^* \xrightarrow{k_{bb}} R_n^{***}$$

d. β scission reactions ($n > 3$)

$$R_n^{***} \xrightarrow{k_\beta} U_3 + R_{n-3}^*$$
$$R_n^{***} \xrightarrow{k_\beta} U_{n-2} + R_2^*$$
$$R_n^{**} \xrightarrow{k_\beta} U_{n-m} + R_m^*$$
$$R_n^{**} \xrightarrow{k_\beta} U_m + R_{n-m}^*$$

e. Intermolecular chain transfer to polymer reactions

$$R_n^* + D_m \xrightarrow{k_{trP}} D_n + R_m^{**}$$
$$R_n^* + U_m \xrightarrow{k_{trP}} D_n + R_m^{**}$$

f. Chain transfer to monomer reactions

$$R_n^* + M \xrightarrow{k_{trM}} D_n + R_1^*$$
$$R_n^{**} + M \xrightarrow{k_{trM}^t} D_n + R_1^*$$
$$R_n^{***} + M \xrightarrow{k_{trM}^t} D_n + R_1^*$$

g. Chain transfer to solvent reactions

$$R_n^* + S \xrightarrow{k_{trS}} D_n + R_0^*$$
$$R_n^{**} + S \xrightarrow{k_{trS}^t} D_n + R_0^*$$
$$R_n^{***} + S \xrightarrow{k_{trS}^t} D_n + R_0^*$$

h. Termination by coupling reactions

$$R_n^* + R_m^* \xrightarrow{k_{tc}} D_{n+m}$$
$$R_n^* + R_m^{**} \xrightarrow{k_{tc}^t} D_{n+m}$$
$$R_n^* + R_m^{***} \xrightarrow{k_{tc}^t} D_{n+m}$$
$$R_n^{**} + R_m^{**} \xrightarrow{k_{tc}^{tt}} D_{n+m}$$
$$R_n^{**} + R_m^{***} \xrightarrow{k_{tc}^{tt}} D_{n+m}$$
$$R_n^{***} + R_m^{***} \xrightarrow{k_{tc}^{tt}} D_{n+m}$$

i. Termination by disproportionation reactions

$$R_n^* + R_m^* \xrightarrow{k_{td}} D_n + U_m$$
$$R_n^* + R_m^{**} \xrightarrow{k_{td}^t} D_n + U_m$$
$$R_n^* + R_m^{***} \xrightarrow{k_{td}^t} D_n + U_m$$
$$R_n^{**} + R_m^{**} \xrightarrow{k_{td}^{tt}} D_n + U_m$$
$$R_n^{**} + R_m^{***} \xrightarrow{k_{td}^{tt}} D_n + U_m$$
$$R_n^{***} + R_m^{***} \xrightarrow{k_{td}^{tt}} D_n + U_m$$

double bond. R_n^* is a secondary radical with n monomer units. R_n^{**} is a tertiary radical with n monomer units formed by the intermolecular chain transfer to polymer reactions. R_n^{***} represents a tertiary radical with n monomer units generated by the backbiting reactions. SCB denotes a short branching point, and LCB a long chain branching point.

The self-initiation reaction is considered to occur via the diradical mechanism of self-initiation reported in [10]. The overall self-initiation reaction is included in the mechanism given above. It follows a second order reaction. The secondary radicals formed by the self-initiation reaction react with a monomer, leading to chain propagation. Tertiary radicals formed via chain transfer to polymer and backbiting either propagates to form short chain branches or undergo β-scission. A β-scission reaction generates a dead polymer with a terminal double bond and a secondary radical. The β-scission reactions attribute to lowering of the polymer chain length and the average molecular weights.

B. Rate Equations

On the basis of the reaction mechanisms listed in Table 1, assuming elementary reactions one can derive rate expressions for the various species involved. The production rates of M, S, R_0^*, R_1^*, R_2^*, R_3^*, R^*, R^{**}, R^{***}, D and U, respectively, are:

$$\begin{aligned}
r_M = \; & -3k_i[M]^2 - k_p[M][R^*] - k_p^t[M]([R^{**}] + [R^{***}]) \\
& -k_{tr_M}[M][R^*] - k_{tr_M}^t[M]([R^{**}] + [R^{***}])
\end{aligned}$$

$$r_S = \; -k_{tr_S}[S][R^*] - k_{tr_S}^t[S]([R^{**}] + [R^{***}])$$

$$\begin{aligned}
r_{R_0^*} = \; & k_{tr_S}[S][R^*] + k_{tr_S}^t[S]([R^{**}] + [R^{***}]) \\
& -k_p[M][R_0^*] - k_{mac}[R_0^*][U] - 0.5k_t[R^*][R_0^*] \\
& -0.5k_t^t([R^{***}] + [R^{**}])[R_0^*]
\end{aligned}$$

$$\begin{aligned}
r_{R_1^*} = \; & k_i[M]^2 + k_p[M]([R_0^*] - [R_1^*]) + k_{tr_M}[M]([R^*] \\
& -R_1^*]) + k_{tr_M}^t[M]([R^{**}] + [R^{***}]) - k_{tr_S}[S][R_1^*] \\
& -k_{mac}[U][R_1^*] - 0.5k_t[R^*][R_1^*] - 0.5k_t^t([R^{***}] \\
& +[R^{**}])[R_1^*] - k_{tr_P}[R_1^*]([U] + [D])
\end{aligned}$$

$$\begin{aligned}
r_{R_2^*} = \; & k_i[M]^2 + k_p[M]([R_1^*] - [R_2^*]) + k_\beta[R^{***}] \\
& -k_{mac}[U][R_2^*] - k_{tr_P}([D] + [U])[R_2^*] \\
& -(k_{tr_M}[M] + k_{tr_S}[S])[R_2^*] - 0.5k_t[R^*][R_2^*] \\
& -0.5k_t^t([R^{***}] + [R^{**}])[R_2^*]
\end{aligned}$$

$$\begin{aligned}
r_{R_3^*} = \; & k_p[M]([R_2^*] - [R_3^*]) - k_{mac}[U][R_3^*] - k_{tr_P}([D] \\
& +[U])[R_3^*] - (k_{tr_M}[M] + k_{tr_S}[S])[R_3^*] \\
& -0.5k_t[R^*][R_3^*] - 0.5k_t^t([R^{***}] + [R^{**}])[R_3^*]
\end{aligned}$$

$$\begin{aligned}
r_{R^*} = \; & 2k_i[M]^2 + k_p^t[M]([R^{**}] + [R^{***}]) - k_{mac}[U][R^*] \\
& -k_{bb}[R^*] + 2k_\beta([R^{***}] + [R^{**}]) - k_{tr_P}([D] \\
& +[U])[R^*] + (k_{tr_M}^t[M] + k_{tr_S}^t[S])([R^{**}] \\
& +[R^{***}]) - k_t[R^*]^2 - 0.5k_t^t([R^{***}] + [R^{**}])[R^*]
\end{aligned}$$

$$\begin{aligned}
r_{R^{**}} = \; & -k_p^t[M][R^{**}] - 2k_\beta[R^{**}] + k_{tr_P}([D] + [U])[R^*] \\
& -(k_{tr_M}^t[M] + k_{tr_S}^t[S])[R^{**}] - 0.5k_t^t[R^*][R^{**}] \\
& -0.5k_t^{tt}(2[R^{**}] + [R^{***}])[R^{**}] + k_{mac}[U][R^*]
\end{aligned}$$

$$\begin{aligned}
r_{R^{***}} = \; & -k_p^t[M][R^{***}] + k_{bb}[R^*] - 2k_\beta[R^{***}] \\
& -(k_{tr_M}^t[M] + k_{tr_S}^t[S])[R^{***}] - 0.5k_t^t[R^*] \\
& [R^{***}] - 0.5k_t^{tt}([R^{**}] + 2[R^{***}])[R^{***}]
\end{aligned}$$

$$\begin{aligned}
r_D = \; & k_{tr_P}[R^*][U] + (k_{tr_M}[M] + k_{tr_S}[S])[R^*] \\
& +(k_{tr_M}^t[M] + k_{tr_S}^t[S])([R^{**}] + [R^{***}]) \\
& +0.5k_t[R^*]^2 + 0.5k_t^t[R^*]([R^{**}] + [R^{***}]) \\
& +0.5k_t^{tt}([R^{**}][R^{***}] + [R^{**}]^2 + [R^{***}]^2)
\end{aligned}$$

$$\begin{aligned}
r_U = \; & 2k_\beta([R^{**}] + [R^{***}]) - k_{tr_P}[R^*][U] \\
& -k_{mac}[R^*][U] + 0.5k_{t_d}[R^*]^2 + 0.5k_{t_d}^t[R^*] \\
& ([R^{**}] + [R^{***}]) + 0.5k_{t_d}^{tt}([R^{**}][R^{***}] \\
& +[R^{**}]^2 + [R^{***}]^2)
\end{aligned}$$

where $[z]$ denotes the molar concentration of species z, R^* is a secondary radical, R^{**} is a tertiary radical formed by the intermolecular chain transfer to polymer reactions, and R^{***} represents a tertiary radical generated by the backbiting reactions.

C. Batch Reactor Model

Mole balances for all species involved yield a mathematical model of the batch reactor:

$$\begin{aligned}
\frac{d[M]}{dt} &= r_M, & [M](0) &= [M]_0 \\
\frac{d[S]}{dt} &= r_S, & [S](0) &= [S]_0 \\
\frac{d[R_0^*]}{dt} &= r_{R_0^*}, & [R_0^*](0) &= 0 \\
\frac{d[R_1^*]}{dt} &= r_{R_1^*}, & [R_1^*](0) &= 0 \\
\frac{d[R_2^*]}{dt} &= r_{R_2^*}, & [R_2^*](0) &= 0 \\
\frac{d[R_3^*]}{dt} &= r_{R_3^*}, & [R_3^*](0) &= 0 \\
\frac{d[R^*]}{dt} &= r_{R^*}, & [R^*](0) &= 0 \\
\frac{d[R^{**}]}{dt} &= r_{R^{**}}, & [R^{**}](0) &= 0 \\
\frac{d[R^{***}]}{dt} &= r_{R^{***}}, & [R^{***}](0) &= 0 \\
\frac{d[D]}{dt} &= r_D, & [D](0) &= 0 \\
\frac{d[U]}{dt} &= r_U, & [U](0) &= 0
\end{aligned}$$

where $[M]_0$ and $[S]_0$ are the initial concentrations of M and S, respectively. The number-average molecular weight of the dead polymer chains, M_n, and the monomer conversion, X, are then obtained from:

$$\begin{aligned}
M_n &= \frac{[M]_0 - [M]}{[D] + [U]} M_m \\
X &= 1 - \frac{[M]}{[M]_0}
\end{aligned}$$

TABLE II

REACTION RATE CONSTANT VALUES.

Parameter	Frequency Factor		Activation Energy $kJ.mol^{-1}$	Ref.
k_p	2.21×10^7	$L.mol^{-1}.s^{-1}$	17.9	[28]
k_p^t	1.2×10^6	$L.mol^{-1}.s^{-1}$	28.6	[29]
k_{bb}	7.41×10^7	s^{-1}	32.7	[30]
k_{tr_M}	2.9×10^5	$L.mol^{-1}.s^{-1}$	32.6	[12]
k_t	3.89×10^9	$L.mol^{-1}.s^{-1}$	8.4	[31]
k_t^{tt}	5.3×10^9	$L.mol^{-1}.s^{-1}$	19.6	[13]
k_β	1.49×10^9	s^{-1}	63.9	[13]
k_{tr_P}	4.01×10^3	$L.mol^{-1}.s^{-1}$	29.0	[32]
C_{tr_S}	107		35.4	[13]

TABLE III

OTHER KINETIC PARAMETER VALUES [13].

Parameter	Dimensionless Value
δ_s	0.1
δ_{st}	0.7
δ_t	0.9
γ	0.5

III. PARAMETER ESTIMATION

Parameter estimation was carried out using least-squared-error minimization and measurements of monomer conversion from isothermal spontaneous thermal polymerization of nBA (40 wt% nBA and 60 wt% xylene) at 140 and 160°C [8]. The minimization was conducted using the optimization routine `fminsearch` from the Optimization Toolbox of MATLAB R2010b. Except for the frequency factor and activation energy of the self-initiation reaction that were estimated in this study, the other reaction kinetic parameter values were taken from the literature (Table 2). Two difference sets of conversion measurements (set 1 and set 2) were used in this study. Each set included gravimetric measurements of monomer conversion from isothermal batch operations at 140 and 160°C.

First, the self-initiation reaction rate constant at 140°C was estimated from set-1 conversion measurements obtained at 140°C. Second, the self-initiation reaction rate constant at 160°C was estimated from set-1 conversion measurements from batch operations at 160°C. Third, using the Arrhenius plot, the frequency factor and activation energy of the self-initiation reaction were calculated:

$$\begin{aligned} \text{Activation Energy} &= 47.901 && kJ.mol^{-1} \\ \text{Frequency Factor} &= 4.810 \times 10^{-4} && L.mol^{-1}.s^{-1} \end{aligned}$$

The quality of the model fitting the conversion data set 1 can be seen in Figures 1 and 2. The second set of conversion data (set 2) at 140 and 160°C was then used for the model validation. The validation results are shown in Figures 3 and 4; as can be seen, the model predicts the conversion reasonably well.

IV. BATCH REACTOR OPTIMIZATION

Using the reactor model presented in Section IIIB, we calculated an optimal temperature profile, $T^*(t)$, for a batch

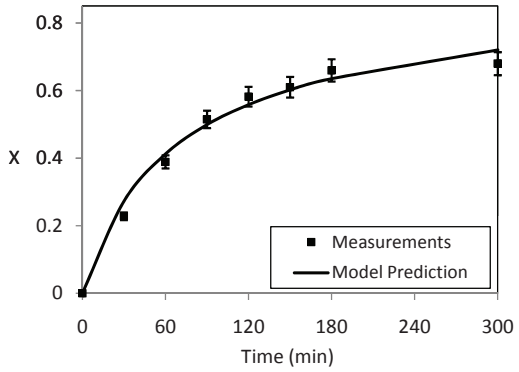

Fig. 1. Model prediction fitted to the measurement set 1 at 140°C

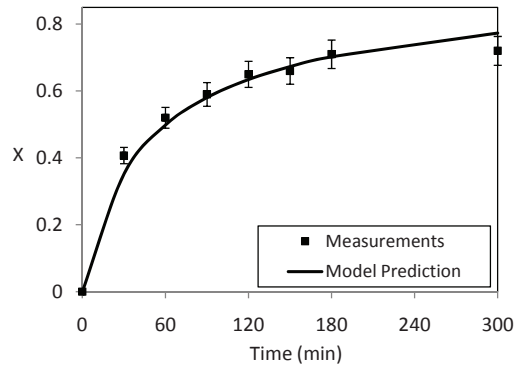

Fig. 2. Model prediction fitted to the measurement set 1 at 160°C

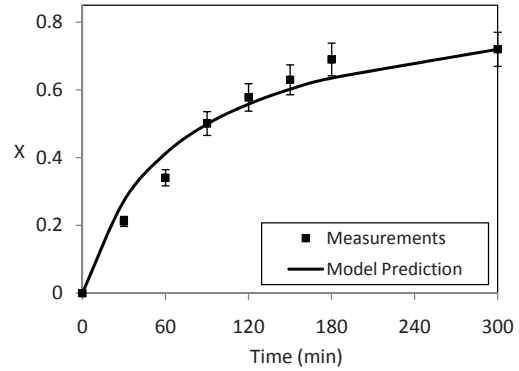

Fig. 3. Model validation: model prediction and measurement set 2 at 140°C

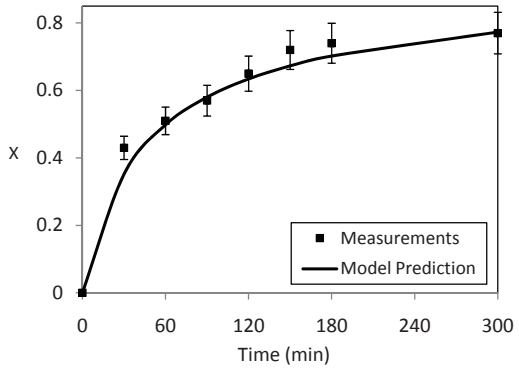

Fig. 4. Model validation: model prediction and measurement set 2 at 160°C

TABLE IV

REACTION RATE CONSTANT DEFINITIONS/RELATIONS.

k_t	$= k_{t_c} + k_{t_d}$	
k_t^t	$= k_{t_c}^t + k_{t_d}^t$	
k_t^{tt}	$= k_{t_c}^{tt} + k_{t_d}^{tt}$	
k_{t_d}	$= \delta_s k_t$	[13]
$k_{t_d}^{tt}$	$= \delta_t k_t^{tt}$	[13]
$k_{t_d}^t$	$= \delta_{st}\sqrt{k_t k_t^{tt}}$	[13]
k_{t_c}	$= (1-\delta_s)k_t$	[13]
$k_{t_c}^{tt}$	$= (1-\delta_t)k_t^{tt}$	[13]
$k_{t_c}^t$	$= (1-\delta_{st})\sqrt{k_t k_t^{tt}}$	[13]
k_{tr_S}	$= C_{tr_S} k_p$	
$k_{tr_M}^t$	$= \frac{k_p^t}{k_p} k_{tr_M}$	[13]
$k_{tr_S}^t$	$= \frac{k_p^t}{k_p} k_{tr_S}$	[13]
k_{mac}	$= \gamma k_p$	[13]

nBA polymerization reactor with a batch cycle time of 7 hours (including the heating-up and cooling-down periods). The batch reactor temperature should be 295.2 K at the beginning and the end of each batch cycle; $T^*(0) = 295.2\ K$ and $T^*(7\times 3600) = 295.2\ K$. The reactor is initially loaded with monomer (40 wt.%) and solvent (60 wt.%). The optimal temperature profile should minimize the performance index:

$$[1 - X(t_f)]^2 + \left[1 - \frac{M_n(t_f)}{5000}\right]^2$$

where $t_f = 7 \times 3600\ s$. In other words, the optimal temperature profile should yield a polymer product with a monomer conversion and a number-average molecular weight as close as possible to one and $5,000\ kg.kmol^{-1}$, respectively.

To simplify the optimization problem, we parameterized the reactor temperature profile using a fourth-order polynomial in time; that is,

$$T^*(t) = at^4 + bt^3 + ct^2 + dt + e$$

where

$$e = 295.2\ K,$$

$$d = -(at_f^3 + bt_f^2 + ct_f)\ K.s^{-1}$$

This parameterization of the optimal temperature profile reduced the search for an optimal profile to a search for three constants, $a,\ b$ and c.

The optimization routine `fminsearch` from the Optimization Toolbox of MATLAB R2010b with the initial guesses:

$$a = -1.118 \times 10^{-14}$$
$$b = +5.634 \times 10^{-10}$$
$$c = -9.743 \times 10^{-6}$$

was used to calculate the optimal values of $a,\ b$ and c. These initial guesses correspond to the initial-guess temperature profile shown in Figure 5.

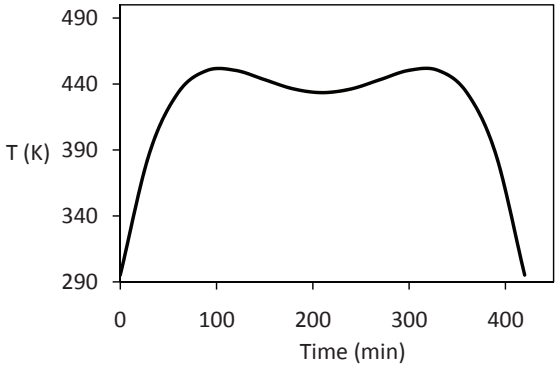

Fig. 5. Initial guess for the reactor temperature profile

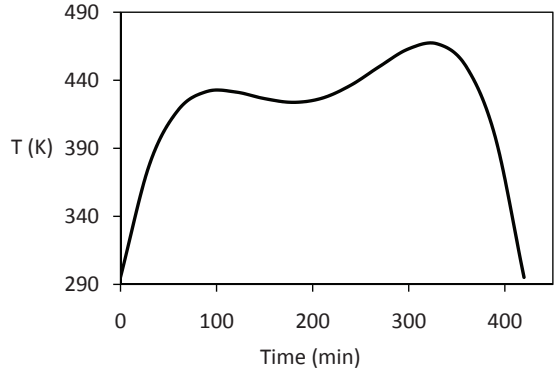

Fig. 6. Optimal reactor temperature profile

The optimization routine calculated the optimal values:

$$a = -1.1792621 \times 10^{-14}$$
$$b = +5.7145938 \times 10^{-10}$$
$$c = -9.3248464 \times 10^{-6}$$

which correspond to the optimal temperature profile shown in Figure 6. Enforcing the optimal temperature profile to the reactor leads to the production of a polymer with $X(t_f) = 0.814$ and $M_n(t_f) = 4918\ kg.kmol^{-1}$.

The optimization results shown herein were for a batch reactor; they were presented to just show an application of the model. A realistic case is that of a semi-batch reactor in which the monomer is added to the reactor over time such that the mass fraction of free (unreacted) monomer in the reactor never exceeds 10%. This upper limit on the monomer mass fraction is to ensure the reactor safety. In this case, the entire solvent is loaded initially, and the optimization variables are the reactor temperature and the monomer feed flow rate.

V. CONCLUSIONS

A macroscopic mechanistic mathematical modeling and optimization study of a batch polymerization reactor in which self-initiated free-radical polymerization of n-butyl acrylate at 140 and 160°C takes place, was presented.

The model was obtained using a comprehensive free-radical polymerization reaction mechanism. The rate constant of the monomer self-initiation was estimated from monomer conversion measurements. The model validation results showed that the macroscopic mechanistic model is accurate enough for optimizing the self-initiated polymerization process to produce high quality acrylic resins. On the basis of the model, optimization was conducted, and an optimal batch-reactor temperature profile that yields an end-batch polymer product with desired properties (conversion and number-average molecular weight) was calculated. Other applications of the model include model-based controller design, reactor scaleup and safety analysis.

VI. Acknowledgement

This material is based upon work supported by the National Science Foundation under Grant No. CBET–0932882. The authors thank Mona Bavarian for her invaluable help with the simulations, and gratefully acknowledge reviewers' comments.

References

[1] Report on Automotive Coatings Adhesives and Sealants, Freedonia Group, May 2008; www.freedoniagroup.com

[2] Cunningham, M.F., Hutchinson, R. Industrial applications and processes. in *Handbook of Radical Polymerization*, K. Matyjaszewski and T. P. Davis, Editors, John Wiley and Sons Inc., Hoboken, NJ, 2002, p 333.

[3] VOC's Directive, EU Committee of the American Chamber of Commerce in Belgium, ASBL/VZw, Brussels, July 8, 1996.

[4] Cheifari, J., Jeffery, J., Mayadunne, R.T.A., Moad G., Rizzardo, E., Thang, S.G., Chain Transfer to Polymer: A Convenient Route to Macromonomers, *Macromolecules*, vol. 32, 1999, p 7700.

[5] Peter, A.C. Moskal, M.G. www.arkema-inc.com/literature/pdf/304/pdf Arkema Inc., King of Prussia, PA.

[6] Grady, M.C., Quan, C., Soroush, M., Thermally initiated polymerization process. US Patent Application Number 60/484,393, filed on July 2, 2003.

[7] Quan, C., Soroush, M., Grady, M.C., Hansen, J.E., Simonsick, W.J., Characterization of Thermally Polymerized n-Butyl Acrylate and Ethyl Acrylate, *Macromolecules*, vol. 38, 2005, pp 76197628.

[8] Rantow, F.S., Soroush M., Grady, M.C., Kalfas, G.A., Spontaneous Polymerization and Chain Microstructure Evolution in High-Temperature Solution Polymerization of n-Butyl Acrylate, *Polymer*, vol. 47, 2006, pp 1423–1435.

[9] Srinivasan, S. , Lee, M.W , Grady, M.C., Soroush, M., Rappe, A.M., Computational Study of Self-initiation Mechanism in Thermal Polymerization of Methyl Acrylate, *J. Phys. Chem. A*, vol. 113, 2009, pp 1078710794.

[10] Srinivasan, S., Lee, M.W., Grady, M.C., Soroush, M., Rappe, A.M., Self-Initiation Mechanism in Spontaneous Thermal Polymerization of Ethyl an n-Butyl Acrylate: a Theoretical Study, *J. Phys. Chem. A*, vol. 114, 2010, pp 7975–7983.

[11] Srinivasan, S., Kalfas, G.A., Petkovska, V.I., Bruni, C., Grady, M.C., Soroush, M., Experimental study of the spontaneous thermal homopolymerization of methyl and n-butyl acrylate, J. Appl. Pol. Sci., Vol. 118, 2010, pp 1898–1909.

[12] Maeder, S., Gilbert, R.G., Measurement of Transfer Constant for Butyl Acrylate Free-Radical Polymerization, *Macromolecules,* vol. 33, 1998, pp 4410–4418.

[13] Nikitin, A.N., Hutchinson, R.A., Wang, W., Kalfas, G.A., Richards, J.R., Bruni, C., Effect of Intramolecular Transfer to Polymer on Stationary Free-Radical Polymerization of Alkyl Acrylates, 5 – Consideration of Solution Polymerization up to High Temperatures, *Macromolecular Reaction Engin.*, vol. 4, 2010, pp 691–706.

[14] Wang, W., Nikitin, A., Hutchinson, R., Consideration of Macromonomer Reactions in n-Butyl Acrylate Free Radical Polymerization, *Macromol. Rapid Commn.*, 2009, vol. 30, pp 2022–2027.

[15] Arzamendi, G., Plessis, C., Leiza, J., Asua, J., Effect of the Intramolecular Chain Transfer to Polymer on PLP/SEC Experiments of Alkyl Acrylates. *Macromolecular Theory and Simulations*, vol. 12, 2003, pp 315–324.

[16] Hakim, M., Verhoeven, V., McManus, N.T., Dube, M.A., Penlidis, A. High-Temperature Solution Polymerization of Butyl Acrylate/Methyl Methacrylate: Reactivity Ratio Estimation, *J. Appl. Poly. Sci.*, vol. 77, 2000, pp 602–609.

[17] Villermaux, J.; Blavier, L., Free Radical Polymerization Engineering–I: A New Method for Modeling Free Radical Homogeneous Polymerization Reactions, *Chem. Eng. Sci.*, vol. 39, 1984, pp 87–99.

[18] Gilbert, R.G., Critically-Evaluated Propagation Rate Coefficients in Free Radical Polymerizations I. Styrene and Methyl Methacrylate, *Pure & Appl. Chem.*, vol. 68, 1996, pp 1491–1494.

[19] Asua, J.M., Beuermann, S., Buback, M., Castignolles, P., Charleux, B., Gilbert, R.G., Hutchinson, R.A., Leiza, J.R., Nikitin, A.N., Vairon, J. P., Van Herk, A.M., Critically Evaluated Rate Coefficients for Free Radical Polymerizations, Propagation Rate Coefficient for Butyl Acrylate, *Macromol. Chem.*, vol. 205, 2004, pp 2151–2160.

[20] Willemse, R.X.E., Van Herk, A.M., Panchenko, E., Junkers, T., Buback, M., PLP-ESR Monitoring of Midchain Radicals in n-Butyl Acrylate Polymerization, *Macromolecules*, 2005, 38, pp 5098–5103.

[21] Pryor, W.A., Lasswell, L.D., *Advances in free radical chemistry*, Academic Press, New York, 1975, Vol. V.

[22] Stickler, M., Meyerhoff, G., The Spontaneous Thermal Polymerization of Methyl Methacrylate. 5. Experimental Study and Computer Simulation of the High Conversion Reaction at 130°C, *Polymer*, vol. 22, 1981, pp 928–933.

[23] Blavier, L., Villermaux, J., Free Radical Polymerization Engineering–II: Modeling of Homogeneous Polymerization of Styrene in a Batch Reactor, Influence of Initiator. *Chem. Eng. Sci.* vol. 39, 1984, pp 101–110.

[24] Peck, A.N.F., Hutchinson, R.A., Grady, M.C., Branching and Scission Reactions in High Temperature Acrylate Polymerizations, *Polymer Preprints*, vol. 43, 2002, p 154.

[25] Peck, A.N.F., Hutchinson, R.A., Secondary Reactions in the High Temperature Free Radical Polymerization of Butyl Acrylate, *Macromolecules*, vol. 37, 2004, pp 5944–5951.

[26] Subrahmanyam, B., Baruah, S.; Rahman, M., Laskar, N., Mazumder, R., Studies on High Conversion Polymerization of n-Alkyl Acrylates, *Polymer*, vol. 35 1994, pp 862–865.

[27] Willemse, R.X.E, van Herk, A.M., Determination of Propagation Rate Coefficients of a Family of Acrylates with PLP-MALDI-ToF-MS, *Macromol. Chem. and Phy.*, vol. 211, 2010, pp 539–545.

[28] Asua, J.M., Beuermann, S., Buback, M., Castignolles, P., Charleux, B., Gilbert, R.G., Hutchinson, R., Leiza, J.R., Nikitin, A.N., Vairon, J.P., van Herk, A.M., Critically Evaluated Rate Coefficients for Free-Radical Polymerization, 5 Propagation Rate Coefficient for Butyl Acrylate, *Macromol. Chem. Phys.*, vol. 205(16), 2004, pp 2151–2160.

[29] Hesse, P., *Ph.D. Thesis*, University of Gottingen, 2008.

[30] Nikitin, A.N., Hutchinson, R.A., Wang, W., Kalfas, G.A., Richards, J.R., Bruni, C., The Effect of Intramolecular Transfer to Polymer on Stationary Free-Radical Polymerization of Alkyl Acrylates: 3. Consideration of Solution Polymerization up to High Conversions, *Macromolecular Theory and Simulations*, vol. 4, 2009, pp 247–258.

[31] Nikitin, A.N., Hutchinson, R.A., Polymerization of Alkyl Acrylates: 2. Improved Consideration of Termination, *Macromolecular Theory and Simulations*, vol. 15, 2006, pp 128–136.

[32] Arzamendi, G., Plessis, C., Leiza, J.R., Asua, J.M., Effect of the Intramolecular Chain Transfer to Polymer on PLP/SEC Experiments of Alkyl Acrylates, *Macromolecular Theory and Simulations*, vol. 12, 2003, pp 315–324.